

Fractal dimension of spin glasses interfaces in dimensions $d = 2$ and $d = 3$ via strong disorder renormalization at zero temperature

Cécile Monthus
*Institut de Physique Théorique,
 CNRS and CEA Saclay
 91191 Gif-sur-Yvette, France*

For Gaussian Spin Glasses in low dimensions, we introduce a simple Strong Disorder renormalization procedure at zero temperature. In each disordered sample, the difference between the ground states associated to Periodic and Anti-Periodic boundary conditions defines a system-size Domain Wall. The numerical study in dimensions $d = 2$ (up to sizes 2048^2) and $d = 3$ (up to sizes 128^3) yields fractal Domain Walls of dimensions $d_s(d = 2) \simeq 1.27$ and $d_s(d = 3) \simeq 2.55$ respectively.

I. INTRODUCTION

Within the droplet scaling theory of classical spin-glasses in finite dimensions $d[1-3]$, the two universal critical exponents that characterize the zero-temperature fixed point can be defined by considering, in each disordered sample \mathcal{J} of volume L^d , the two ground states associated to two different boundary conditions, for instance Periodic (P) and Anti-Periodic (AP). The difference between the two ground states defines a system-size Domain-Wall :

(i) the scaling of its energy E^{DW} with respect to the linear size L defines the droplet or stiffness exponent θ

$$E_{\mathcal{J}}^{DW} \equiv E_{\mathcal{J}}^{GS(AP)} - E_{\mathcal{J}}^{GS(P)} = L^{\theta} u \quad (1)$$

where u is an $O(1)$ random variable of zero mean. The numerical values measured in dimensions $d = 2$ and $d = 3$ read (see [4] and references therein)

$$\begin{aligned} \theta(d = 2) &\simeq -0.28 \\ \theta(d = 3) &\simeq 0.24 \end{aligned} \quad (2)$$

(ii) the scaling of its surface Σ^{DW} (number of bonds belonging to the domain wall) defines the fractal dimension d_s of the Domain-Wall

$$\Sigma_{\mathcal{J}}^{DW} \propto L^{d_s} v \quad (3)$$

where v is an $O(1)$ positive random variable. The numerical values measured in dimensions $d = 2$ [5–11] and $d = 3$ [12, 13] read

$$\begin{aligned} d_s(d = 2) &\simeq 1.28 \\ d_s(d = 3) &\simeq 2.58 \end{aligned} \quad (4)$$

Moreover in dimension $d = 2$, the Domain-Wall of fractal dimension $d_s \simeq 1.28$ has been characterized as an SLE process [9, 10]. The fractal dimension d_s plays in particular a major role in the chaos properties of spin-glasses with respect to temperature and to disorder perturbations [2, 3], as well as in the dynamics [14].

From the point of view of real-space renormalization, spin-glasses have been mostly studied within the Migdal-Kadanoff approximation [15–28] where the hypercubic lattice is effectively replaced by a hierarchical fractal lattice whose structure is exactly renormalizable by construction [29–31] : this approximation reproduces very well the values of the droplet exponent in dimensions $d = 2$ and $d = 3$ (Eq 2), but not the surface dimension which is fixed to the trivial value

$$d_s^{MK} = d - 1 \quad (5)$$

If one insists on keeping the hypercubic lattice in dimension $d > 1$, the precise definition of an appropriate renormalization procedure has remained very difficult. The reason can be understood by considering a standard Block Renormalization using the maximal Block size $b = \frac{L}{2}$: if one decomposes the volume L^d into 2^d blocks of volume $(\frac{L}{2})^d$ and compute the ground states in each block, the residual coupling between two blocks is the sum over $(\frac{L}{2})^{d-1}$ initial couplings of random signs, leading to the too high value

$$\theta^{Block} = \frac{d-1}{2} \quad (6)$$

This poor value comes from the facts that the Domain-Walls have been assumed to be of dimension

$$d_s^{Block} = d - 1 \quad (7)$$

and have been fixed at the middle of the sample independently of the disorder realization. To obtain better results, it is thus necessary to build correlated clusters with boundaries adapted to each disorder realization. In the present paper, we thus introduce and study numerically some simple Strong Disorder real-space renormalization in dimensions $d = 2$ and $d = 3$, and obtain that it is able to reproduce very well the fractal dimensions d_s quoted in Eq. 4.

The paper is organized as follows. The principle of the Strong Disorder real-space renormalization at zero temperature is described in section II. The numerical application in dimension $d = 2$ and $d = 3$ are presented in sections III and IV respectively. Our conclusions are summarized in section V.

II. STRONG DISORDER RENORMALIZATION AT ZERO TEMPERATURE

For a finite-dimensional spin-glass of Hamiltonian

$$H = - \sum_{(i,j)} J_{ij} S_i S_j \quad (8)$$

where $S_i = \pm 1$ are classical spins, and where J_{ij} are the random Gaussian couplings of zero mean, we would like to construct the ground state via some simple strong disorder real-space renormalization procedure.

A. Analysis of the local fields

For each spin S_i , we thus consider its local field

$$h_i^{loc} = \sum_j J_{ij} S_j \quad (9)$$

and compute its largest coupling in absolute value, corresponding to some index $j_{max}(i)$

$$\max_j (|J_{ij}|) \equiv |J_{i,j_{max}(i)}| \quad (10)$$

We ask whether the local field

$$h_i^{loc} = J_{i,j_{max}(i)} S_{j_{max}(i)} + \sum_{j \neq j_{max}(i)} J_{ij} S_j \quad (11)$$

can be dominated by the first term whatever the values taken by the spins S_j of the second term.

B. Comparison with the worst case

The 'worst case' is of course when all the spins S_j of the second term in Eq. 11 are such that $(J_{ij} S_j)$ all have the same sign, so that their contribution to the local field is maximal. It is thus convenient to introduce the difference

$$\Delta_i \equiv |J_{i,j_{max}(i)}| - \sum_{j \neq j_{max}(i)} |J_{ij}| \quad (12)$$

If $\Delta_{i_0} > 0$, the sign of the local field $h_{i_0}^{loc}$ will be determined by the sign of the first term $J_{i_0 j_{max}(i_0)} S_{j_{max}(i_0)}$ for all values taken by the other spins S_j with $j \neq j_{max}(i_0)$

$$\text{sgn}(h_{i_0}^{loc}) = S_{j_{max}(i_0)} \text{sgn}(J_{i_0, j_{max}(i_0)}) \quad (13)$$

Then the spin S_{i_0} can be eliminated via

$$S_{i_0} = S_{j_{max}(i_0)} \text{sgn}(J_{i_0, j_{max}(i_0)}) \quad (14)$$

so that the Hamiltonian of Eq. 8 becomes

$$H = -|J_{i_0 j_{max}(i_0)}| - \sum_{(i,j) \neq i_0} J_{ij}^R S_i S_j \quad (15)$$

where the renormalized couplings concerning the spin $S_{j_{max}(i_0)}$ read

$$J_{j_{max}(i_0),j}^R = J_{j_{max}(i_0),j} + J_{i_0,j} \text{sgn}(J_{i_0 j_{max}(i_0)}) \quad (16)$$

For a site i_0 having coordinence $z = 2$ (i.e. only two neighbors), the difference Δ_{i_0} is always positive, so that the renormalization above is exact : this is the case in particular in dimension $d = 1$ and in the Migdal-Kadanoff approximation in dimension $d > 1$ (see sections 4.2 and 4.3 of Ref [32] for more details).

C. Comparison with the typical case

However “the worst is not always true” : indeed in a frustrated spin-glass, the worst case discussed above where all the spins S_j are such that $(J_{ij} S_j)$ have all the same sign, is expected to be rather atypical. In the absence of other informations, it is much more natural to compare with a sum of random terms of absolute values J_{ij} and of random signs, i.e. to replace the difference Δ_i of Eq. 12 by

$$\Omega_i \equiv |J_{i,j_{max}(i)}| - \sqrt{\sum_{j \neq j_{max}(i)} |J_{ij}|^2} \quad (17)$$

Note that for the case of coordinence $z = 2$, Ω_i actually coincides with Δ_i , so that the exactness discussed above is the same. But for coordinence $z > 2$, we expect that Ω_i is a better indicator of the relative dominance of the maximal coupling for the different spins. We have thus chosen to introduce the Strong Disorder Renormalization procedure based on the variable Ω_i as we now describe.

D. Formulation of Strong Disorder Renormalization procedure

At each step, the spin-glass Hamiltonian of the form of Eq. 8 contains N remaining spins. Each spin S_i is characterized by the variable Ω_i of Eq. 17 computed from the couplings J_{ij} connected to S_i .

The iterative renormalization procedure is defined by the following elementary decimation step :

Find the spin i_0 with the maximal Ω_i

$$\Omega_{i_0} \equiv \max_i(\Omega_i) \quad (18)$$

The elimination of the spin S_{i_0} via the rule of Eq. 14 yields that all its couplings $J_{i_0,j}$ with $j \neq j_{max}(i_0)$ are transferred to the spin $S_{j_{max}(i_0)}$ via the renormalization rule of Eq. 16

$$J_{j_{max}(i_0),j}^R = J_{j_{max}(i_0),j} + J_{i_0,j} \text{sgn}(J_{i_0 j_{max}(i_0)}) \quad (19)$$

The procedure ends when only a single spin S_{last} is left : the two values $S_{last} = \pm 1$ label the two ground states related by a global flip of all the spins. From the choice $S_{last} = +1$, we may reconstruct all the values of the decimated spins via the rule of Eq. 14.

In the sections III and IV, we study numerically this renormalization procedure in dimensions $d = 2$ and $d = 3$ to see whether the corresponding exponents θ and d_s are closer to the numerical values of Eqs 2 and 4 than the block values of Eqs 6 and 7. But let us first mention similarities and differences with previous works.

E. Differences with the ‘greedy’ procedure for classical spin-glasses

The simplest ‘greedy’ procedure introduced for classical spin-glasses consists in satisfying the bonds in the order of the absolute values of the couplings $|J_{i,j}|$ unless a closed loop appears [33–35]. So the two differences with the present procedure is that

(i) here we decimate spins according to the biggest variable Ω_i of Eq. 17, instead of decimating ‘bonds’ according to the biggest $|J_{i,j}|$

(ii) here the couplings are renormalized according to Eq. 19, whereas in the greedy procedure of Refs [33–35], no renormalization is mentioned.

In dimensions $d = 2$ and $d = 3$, the corresponding fractal dimensions of the Domain-Wall have been numerically measured to be $d_f^{greedy}(d = 2) \simeq 1.2 \pm 0.02$ and $d_f^{greedy}(d = 3) \simeq 2.5 \pm 0.05$ [33] (i.e. somewhat slightly lower than Eq. 4 at least in dimension $d = 2$).

In the context of the one-dimensional spin-glasses with power-law couplings $J(r) \propto 1/r^\sigma$, we have studied recently a related strong disorder renormalization procedure able to reproduce the correct droplet exponent [32], using the strong hierarchy of initial couplings with the distance.

F. Differences with Strong Disorder RG for quantum spin-glasses

As a final remark, we should also stress the difference with the strong disorder renormalization method (see [36] for a review) that has been developed for disordered *quantum* spin models either in $d = 1$ [37] or in $d = 2, 3, 4$ [38–48]. In these quantum spin models, the idea is to decimate the strongest coupling J_{max} remaining in the whole system : the renormalized couplings obtained via second order perturbation theory of quantum mechanics are obtained as ratios of couplings and are thus typically much weaker than the decimated coupling J_{max} , so that the procedure is consistent and even asymptotically exact at the critical point where the typical renormalized couplings *decays* as $J_L^{typ} \propto e^{-L^\psi}$. This is thus completely different from the problem of *classical* spin-glasses at zero temperature considered in the present paper, where the droplet scaling is a power-law $J_L \propto L^\theta$, and where the renormalization rule is of the form of Eq. 19, so that it is not easy to know in advance whether the procedure will be consistent or not. In the following sections, we thus present numerical results.

III. APPLICATION TO THE GAUSSIAN SPIN-GLASS IN DIMENSION $d = 2$

A. Numerical procedure

For each disordered sample defined on a square lattice $L \times L$

$$H_{2d} = - \sum_{x=1}^L \sum_{y=1}^L S_{(x,y)} [J_x^P(x,y) S_{(x+1,y)} + J_y^P(x,y) S_{(x,y+1)}] \quad (20)$$

with periodic boundary conditions in the two directions $S_{(L+1,y)} \equiv S_{(1,y)}$ and $S_{(x,L+1)} \equiv S_{(x,1)}$ we apply the renormalization procedure to construct the ground-state configuration $\{S_i^{GS(P)}\}$. As usual, the Anti-Periodic Boundary conditions in the direction x ($S_{(L+1,y)} = -S_{(1,y)}$) can be equivalently studied by changing the signs of the horizontal couplings in the column $x = 1$

$$J_x^{AP}(x = 1, y) = -J_x^P(x = 1, y) \quad (21)$$

The renormalization procedure is again applied to construct the ground-state configuration $\{S_i^{GS(AP)}\}$. The number of bonds having a different satisfaction between the two ground states

$$S_i^{GS(AP)} S_j^{GS(AP)} \text{sgn}(J_{ij}^{AP}) \neq S_i^{GS(P)} S_j^{GS(P)} \text{sgn}(J_{ij}^P) \quad (22)$$

corresponds to the surface $\Sigma_{\mathcal{J}}^{DW}$ of the Domain-Wall (Eq. 3), whereas its energy $E_{\mathcal{J}}^{DW}$ corresponds to the difference between the two ground states energies of Eq. 1.

B. Results in a given sample

As an example, we show on Fig. 1 (a) the interface obtained in a given sample by the procedure described above.

On Fig. 1 (b), we also show the corresponding values of the RG parameter Ω of Eq. 17 as a function of the RG step.

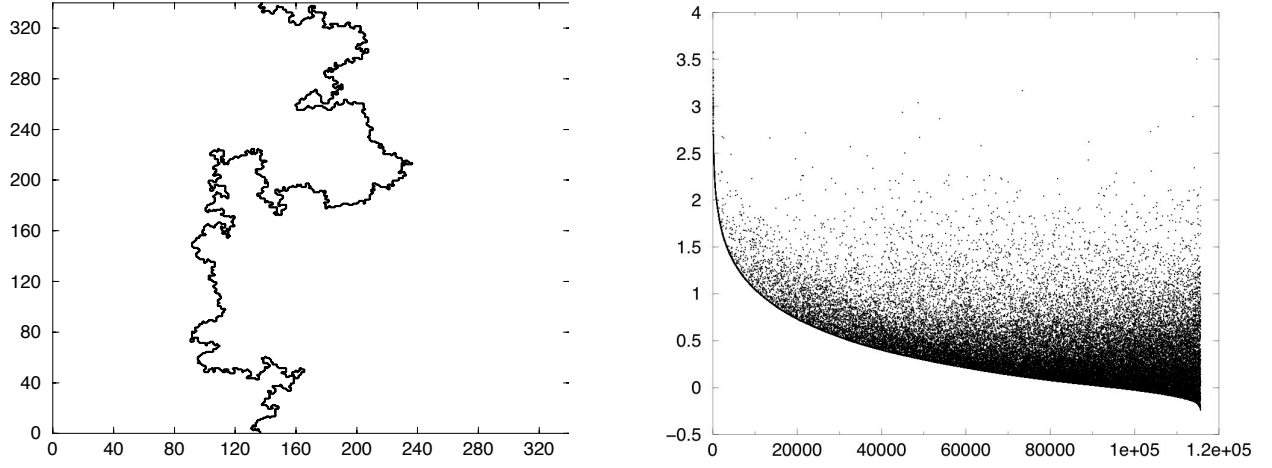


FIG. 1: Strong Disorder Renormalization procedure in a two dimensional sample of size 340×340 :

(a) Domain-Wall between the Periodic and the Anti-Periodic Boundary conditions.

(b) RG parameter Ω of the decimated spin as a function of the RG step (the RG step corresponds to the number of spins that have already been decimated).

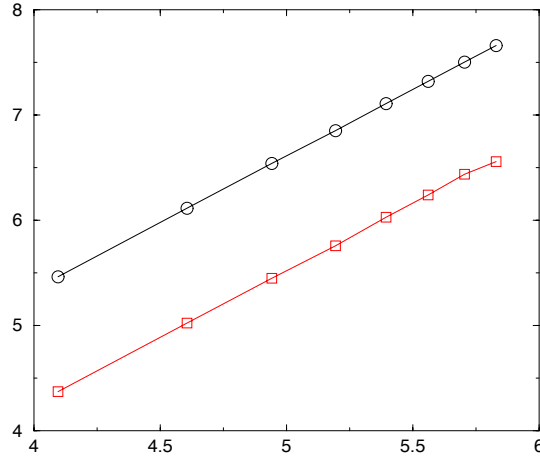


FIG. 2: Log-log plot of the average value $\overline{\Sigma^{DW}}$ (circles) and of the width $\sqrt{(\Sigma^{DW})^2 - (\overline{\Sigma^{DW}})^2}$ (squares) of the length of the Domain-Wall as a function of the size $60 \leq L \leq 340$ of samples : the two slopes correspond to the fractal dimension $d_s \simeq 1.27$.

C. Statistics over disordered samples

The application to $n_s(L)$ independent disordered samples of various sizes L with

$$\begin{aligned} L &= 60, 100, 140, 180, 220, 260, 300, 340 \\ n_s(L) &= 4 \times 10^6, 4 \times 10^5, 8 \times 10^4, 25 \times 10^3, 10^4, 4 \times 10^3, 2 \times 10^3, 12 \times 10^2 \end{aligned} \quad (23)$$

yields that the average value and the width of the length Σ^{DW} of the Domain-Wall have the same scaling (see Fig. 2)

$$\begin{aligned} \overline{\Sigma^{DW}} &\propto L^{d_s} \\ \sqrt{(\Sigma^{DW})^2 - (\overline{\Sigma^{DW}})^2} &\propto L^{d_s} \end{aligned} \quad (24)$$

so that the Domain Wall is a fractal curve of dimension

$$d_s \simeq 1.27 \quad (25)$$

in agreement with the value quoted in Eq. 4 measured via exact numerical methods [5–11].

However the droplet exponent that we measure from the width of the distribution of the Domain-Wall energy E^{DW} (Eq. 1)

$$\sqrt{(E^{DW})^2} \propto L^\theta \quad (26)$$

nearly vanishes $\theta \simeq 0$, i.e. it is far from the correct negative value $\theta(d=2) \simeq -0.28$ quoted in Eq. 2, even if it is not as bad as the positive Block value $\theta^{Block}(d=2) = \frac{1}{2}$ of Eq. 6.

D. Box-variant of the Strong Disorder Renormalization procedure

We have also considered the following Box-variant of the Strong Disorder Renormalization procedure. The initial two-dimensional sample of size $L = 2^n$ is first decomposed into $(\frac{L}{2})^2$ boxes of $2^2 = 4$ spins. We first eliminate in each box the spin with the highest Ω_i in the box, so that there remains three spins per box. We then eliminate again in each box the spin with the highest Ω_i in the box, so that there remains two spins per box. We finally eliminate again in each box the spin with the highest Ω_i in the box, so that there remains one spin per box. We may now group together four boxes to iterate the procedure. This variant allows to consider much bigger sizes L and statistics $n_s(L)$ with respect to Eq. 23

$$\begin{aligned} L &= 2^4, 2^5, 2^6, 2^7, 2^8, 2^9, 2^{10}, 2^{11} \\ n_s(L) &= 6 \times 10^8, 15 \times 10^7, 33 \times 10^6, 75 \times 10^5, 2 \times 10^6, 4 \times 10^5, 7 \times 10^4, 12 \times 10^3 \end{aligned} \quad (27)$$

As an example, we show on Fig. 3 (a) the interface obtained in a given sample of size 2048×2048 . The statistics over samples of length of the Domain-Wall corresponds to the same fractal dimension $d_s \simeq 1.27$ as in Eq. 25.

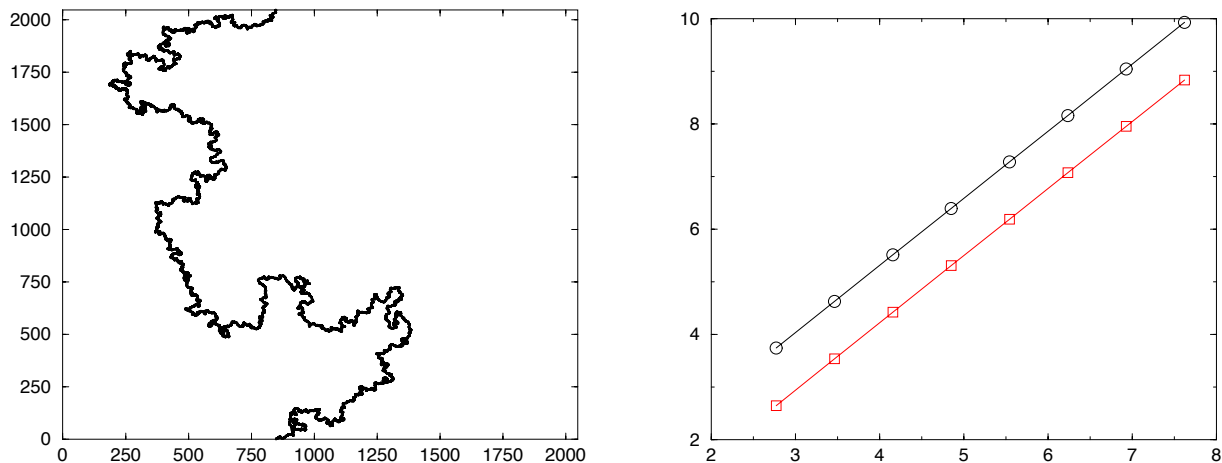


FIG. 3: Box-variant of the Strong Disorder Renormalization procedure in two dimensions :

(a) Domain-Wall between the Periodic and the Anti-Periodic Boundary conditions in a two dimensional sample of size 2048×2048 .

(b) Log-log plot of the average value $\overline{\Sigma^{DW}}$ (circles) and of the width $\sqrt{(\overline{\Sigma^{DW}})^2 - (\overline{\Sigma^{DW}})^2}$ (squares) of the length of the Domain-Wall as a function of the size $2^4 = 16 \leq L \leq 2^{11} = 2048$ of samples : the two slopes correspond to the fractal dimension $d_s \simeq 1.27$ as on Fig. 2.

The corresponding droplet exponent measured from Eq. 26 is slightly negative

$$\theta \simeq -0.09 \quad (28)$$

i.e. it is still far from the correct value $\theta(d=2) \simeq -0.28$ quoted in Eq. 2.

IV. APPLICATION TO THE GAUSSIAN SPIN-GLASS IN DIMENSION $d = 3$

A. Strong Disorder renormalization procedure

For each disordered sample defined on a cubic lattice $L \times L \times L$

$$H_{3d} = - \sum_{x=1}^L \sum_{y=1}^L \sum_{z=1}^L S_{(x,y,z)} [J_x^P(x,y,z)S_{(x+1,y,z)} + J_y^P(x,y,z)S_{(x,y+1,z)} + J_z^P(x,y,z)S_{(x,y,z+1)}] \quad (29)$$

we have applied the same procedure as in $d = 2$ (see details in section III A), the Anti-Periodic boundary conditions corresponding again to the change of the signs of the horizontal couplings in the column $x = 1$

$$J_x^{AP}(x = 1, y, z) = -J_x^P(x = 1, y, z) \quad (30)$$

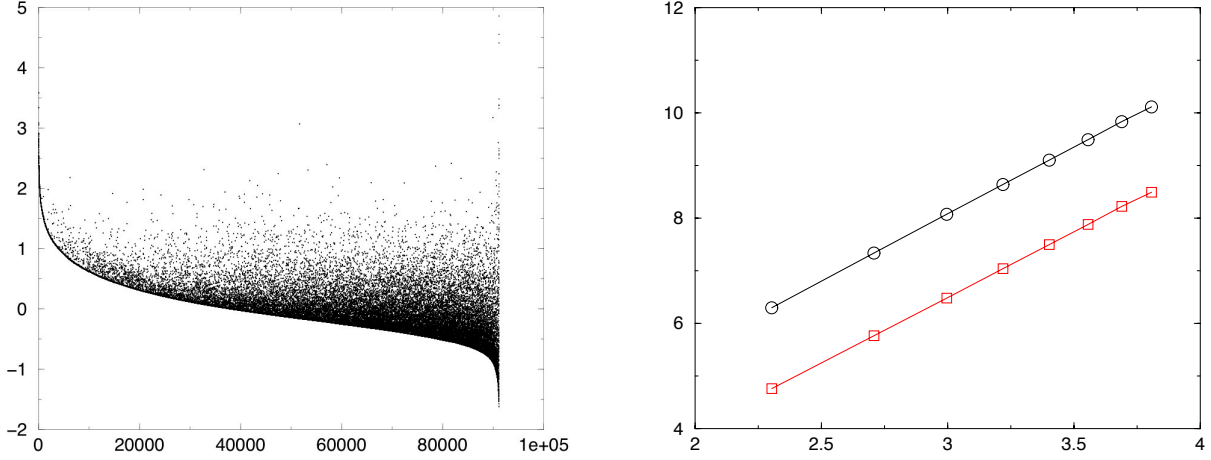


FIG. 4: Strong Disorder RG procedure in $d = 3$

(a) RG parameter Ω of the decimated spin as a function of the RG step (the RG step corresponds to the number of spins that have already been decimated) in a sample of size $45 \times 45 \times 45$.

(b) Log-log plot of the average value $\overline{\Sigma^{DW}}$ (circles) and of the width $\sqrt{(\Sigma^{DW})^2 - (\overline{\Sigma^{DW}})^2}$ (squares) of the surface of the Domain-Wall as a function of the size $10 \leq L \leq 45$ of samples : the slopes correspond to the fractal dimension $d_s \simeq 2.55$.

The application to $n_s(L)$ independent disordered samples of various sizes L with

$$\begin{aligned} L &= 10, 15, 20, 25, 30, 35, 40, 45 \\ n_s(L) &= 21 \times 10^6, 25 \times 10^5, 38 \times 10^4, 10^5, 24 \times 10^3, 9 \times 10^3, 3 \times 10^3, 16 \times 10^2 \end{aligned} \quad (31)$$

yields that the average value and the width of the surface Σ^{DW} of the Domain-Wall have the same scaling (see Fig. 4)

$$\begin{aligned} \overline{\Sigma^{DW}} &\propto L^{d_s} \\ \sqrt{(\Sigma^{DW})^2 - (\overline{\Sigma^{DW}})^2} &\propto L^{d_s} \end{aligned} \quad (32)$$

with the fractal dimension

$$d_s \simeq 2.55 \quad (33)$$

in agreement with the value quoted in Eq. 4 measured via other numerical methods [12, 13].

B. Box-variant of the Strong Disorder renormalization procedure

As in dimension $d = 2$ (see section III D), we have also considered the following Box-variant of the Strong Disorder Renormalization procedure. The initial three-dimensional sample of linear size $L = 2^n$ is first decomposed into $(\frac{L}{2})^3$

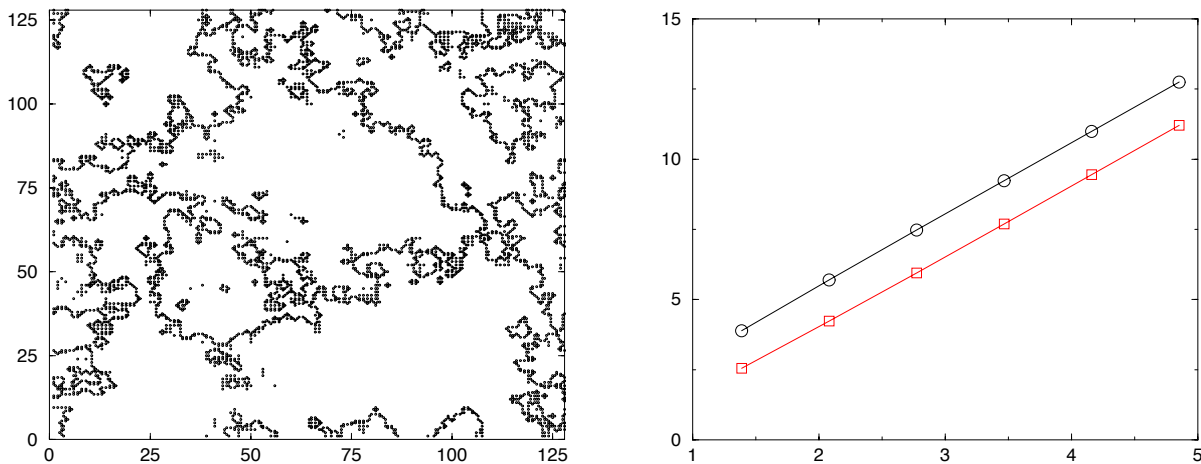


FIG. 5: Box-variant of the Strong Disorder Renormalization procedure in three dimensions :

(a) Cut by the plane $x = \text{constant}$ containing the maximal number of points of the Domain-Wall between the Periodic and the Anti-Periodic Boundary conditions in a given sample of size 128^3 .

(b) Log-log plot of the average value $\overline{\Sigma}^{DW}$ (circles) and of the width $\sqrt{(\overline{\Sigma}^{DW})^2 - (\overline{\Sigma}^{DW})^2}$ (squares) of the surface of the Domain-Wall as a function of the size $2^2 = 4 \leq L \leq 2^7 = 128$ of samples : the slopes correspond to the same fractal dimension $d_s \simeq 2.55$ as on Fig. 4.

boxes of $2^3 = 8$ spins. We perform seven sweeps to decimate iteratively the spin with the highest Ω_i in each box, so that there remains one spin per box. We then group together 8 boxes to iterate the procedure. This variant allows to consider bigger sizes L and statistics $n_s(L)$ with respect to Eq. 31

$$\begin{aligned} L &= 2^2, 2^3, 2^4, 2^5, 2^6, 2^7 \\ n_s(L) &= 15 \times 10^8, 12 \times 10^7, 13 \times 10^6, 10^6, 135 \times 10^3, 8 \times 10^3 \end{aligned} \quad (34)$$

In contrast to $d = 2$ where the Domain-Walls can be easily shown as on Fig. 1 (a), we have not found how to represent clearly the Domain Wall of a given three dimensional sample on a two-dimensional figure. We have thus chosen to show on Fig. 5 (a) the cut of the Domain Wall by the plane $x = \text{constant}$ where the number of points is maximum. As shown on Fig. 5 (b), the statistics over samples of the surface of the Domain-Wall corresponds to the same fractal dimension $d_s \simeq 2.55$ as in Eq. 25.

The droplet exponent that we measure from the width of the distribution of the Domain-Wall energy E^{DW} (Eq. 26)

$$\theta \simeq 0.75 \quad (35)$$

is again far from the correct value $\theta(d = 3) \simeq 0.24$ quoted in Eq. 2, even if it is not as bad as the Block value $\theta^{Block}(d = 3) = 1$ of Eq. 6.

V. CONCLUSION

In summary, we have introduced and studied numerically a simple Strong Disorder renormalization procedure at zero temperature for spin-glasses in dimension $d = 2$ and $d = 3$. Our main conclusion is that it is able to reproduce very well the fractal dimensions d_s quoted in Eq. 4, although it is not able to reproduce the correct droplet exponents of Eq. 2. A possible interpretation is that the fractal dimension d_s is actually determined by the short-scales optimization well captured by the simple Strong Disorder RG procedure, whereas the droplet exponent θ is determined by large-scales optimization that is not well captured by the simple Strong Disorder RG procedure, because the RG parameter Ω remains positive during the first part of the RG steps but tends to become negative in the last part (see Figs 1 (b) and 4). This situation is thus opposite to the Migdal-Kadanoff renormalization, which reproduces very well the droplet exponent θ in dimensions $d = 2$ and $d = 3$, but not the surface fractal dimension d_s (Eq. 5). Let us hope that

in the future it will be possible to formulate an RG procedure able to reproduce both exponents (θ, d_s) correctly!

-
- [1] W.L. Mc Millan, J. Phys. C 17, 3179 (1984).
 - [2] A.J. Bray and M. A. Moore, J. Phys. C 17 (1984) L463; A.J. Bray and M. A. Moore, “Scaling theory of the ordered phase of spin glasses” in Heidelberg Colloquium on glassy dynamics, edited by JL van Hemmen and I. Morgenstern, Lecture notes in Physics vol 275 (1987) Springer Verlag, Heidelberg.
 - [3] D.S. Fisher and D.A. Huse, Phys. Rev. Lett. 56, 1601 (1986) ; Phys. Rev. B 38, 373 (1988) ; Phys. Rev. 38, 386 (1988).
 - [4] S. Boettcher, Eur. Phys. J. B 38, 83 (2004); Phys. Rev. Lett. 95, 197205 (2005).
 - [5] A. J. Bray and M.A. Moore, Phys. Rev. Lett. 58, 57 (1987).
 - [6] A.A. Middleton, Phys. Rev. B 63, 060202(R) (2001).
 - [7] A.K. Hartmann and A.P. Young, Phys. Rev. B 66, 094419 (2002)
 - [8] O. Melchert and A.K. Hartmann, Phys. Rev. B 76, 174411 (2007).
 - [9] C. Amoruso, A.K. Hartmann, M.B. Hastings and M.A. Moore, Phys. Rev. Lett. 97, 267202 (2006).
 - [10] D. Bernard, P. Le Doussal and A.A. Middleton, Phys. Rev. B 76, 020403(R) (2007).
 - [11] S. Risau-Gusman and F. Roma, Phys. Rev. B 77, 134435 (2008).
 - [12] M. Palassini and A.P. Young, Phys. Rev. Lett. 85, 3017 (2000).
 - [13] H.G. Katzgraber, M. Palassini and A.P. Young, Phys. Rev. B 63, 184422 (2001).
 - [14] C. Monthus and T. Garel, J. Phys. A Math Theor 41, 115002 (2008).
 - [15] B.W. Southern and A.P. Young, J. Phys. C 10, 2179 (1977).
 - [16] A. P. Young and R. B. Stinchcombe, J. Phys. C 9 (1976) 4419.
 - [17] S.R. McKay, A.N. Berker and S. Kirkpatrick, Phys. Rev. Lett. 48 (1982) 767;
E. J. Hartford and S.R. McKay, J. Appl. Phys. 70, 6068 (1991).
 - [18] A.J. Bray and M. A. Moore, J. Phys. C 17 (1984) L463.
 - [19] E. Gardner, J. Physique 45, 115 (1984).
 - [20] J.R. Banavar and A.J. Bray, Phys. Rev. B 35, 8888 (1987).
 - [21] M. A. Moore, H. Bokil, B. Drossel, Phys. Rev. Lett. 81 (1998) 4252.
 - [22] M. Nifle and H.J. Hilhorst, Phys. Rev. Lett. 68 (1992) 2992 ;
M. Ney-Nifle and H.J. Hilhorst, Physica A 193 (1993) 48;
M. Ney-Nifle and H.J. Hilhorst, Physica A 194 (1993) 462;
M. Ney-Nifle, Phys. Rev. B 57, 492 (1998).
 - [23] M.J. Thill and H.J. Hilhorst, J. Phys. I France 6, 67 (1996).
 - [24] F. Ricci-Tersenghi and F. Ritort, J. Phys. A: Math. Gen. 33, 3727 (2000).
 - [25] S. Boettcher, Eur. Phys. J. B 33, 439 (2003).
 - [26] C. Monthus and T. Garel, J. Stat. Mech. P01008 (2008).
 - [27] T. Jorg and F. Krzakala, J. Stat. Mech. L01001 (2012).
 - [28] C. Monthus and T. Garel, arXiv:1402.6342.
 - [29] A.A. Migdal, Sov. Phys. JETP 42, 743 (1976) ;
L.P. Kadanoff, Ann. Phys. 100, 359 (1976).
 - [30] A.N. Berker and S. Ostlund, J. Phys. C 12, 4961 (1979).
 - [31] M. Kaufman and R. B. Griffiths, Phys. Rev. B 24, 496 - 498 (1981);
R. B. Griffiths and M. Kaufman, Phys. Rev. B 26, 5022 (1982).
 - [32] C. Monthus, J. Stat. Mech. P06015 (2014).
 - [33] M. Cieplak, A. Maritan and J.R. Banavar, Phys. Rev. Lett. 72, 2320 (1994); M. Cieplak, A. Maritan and J.R. Banavar, Physica A 266, 291 (1999).
 - [34] C.M. Newman and D.L. Stein, Phys. Rev. Lett. 72, 2286 (1994) ;
C.M. Newman and D.L. Stein, J. Stat. Phys. 82, 1113 (1996).
 - [35] T.S. Jackson and N. Read, Phys. Rev. E 81, 021130 (2010).
 - [36] F. Igloi and C. Monthus, Phys. Rep. 412, 277 (2005).
 - [37] D. S. Fisher, Phys. Rev. Lett. 69, 534 (1992); Phys. Rev. B 51, 6411 (1995).
 - [38] D. S. Fisher, Physica A 263, 222 (1999).
 - [39] O. Motrunich, S.-C. Mau, D. A. Huse, and D. S. Fisher, Phys. Rev. B 61, 1160 (2000).
 - [40] Y.-C. Lin, N. Kawashima, F. Igloi, and H. Rieger, Prog. Theor. Phys. 138, 479 (2000).
 - [41] D. Karevski, YC Lin, H. Rieger, N. Kawashima and F. Igloi, Eur. Phys. J. B 20, 267 (2001).
 - [42] Y.-C. Lin, F. Igloi, and H. Rieger, Phys. Rev. Lett. 99, 147202 (2007).
 - [43] R. Yu, H. Saleur, and S. Haas, Phys. Rev. B 77, 140402 (2008).
 - [44] I. A. Kovacs and F. Igloi, Phys. Rev. B 80, 214416 (2009).
 - [45] I. A. Kovacs and F. Igloi, Phys. Rev. B 82, 054437 (2010).
 - [46] I. A. Kovacs and F. Igloi, Phys. Rev. B 83, 174207 (2011).
 - [47] I. A. Kovacs and F. Igloi, Eur. Phys. Lett. 97, 67009 (2012).
 - [48] I. A. Kovacs and F. Igloi, J. Phys. Condens. Matter 23, 404204 (2011).